Grant agreement no:
608571

Project acronym:
SUCCESS

Project full title:
Industrial steam generation with 100% carbon capture and insignificant efficiency penalty – scale-up of oxygen carrier for chemical-looping combustion using environmentally sustainable materials

Collaborative project

Theme:
FP7-ENERGY.2013.5.1.1

Deliverable D4.3

Report on performance and attrition testing on 25 kg batch of spray-dried material

Due delivery date: 2015-08-31
Actual delivery date: 2016-11-21

Lead beneficiary:
Partner no. 2 – Chalmers University of Technology

Dissemination level:
Public (PU)

CHALMERS UNIVERSITY OF TECHNOLOGY	**DELIVERABLE 4.2**

Report on performance and attrition testing on 25 kg batch of spray-dried material

SUCCESS – Industrial steam generation with 100% carbon capture and insignificant efficiency penalty - scale-up of oxygen carrier for chemical-looping combustion using Environmentally sustainable materials	**Keywords:** C28E1S2, perovskite, $CaMn_{0.775}Mg_{0.1}Ti_{0.125}O_{3-\delta}$, spray-drying, continuous operation, 10 kW unit
Work package: 4 – Attrition testing and performance verification of material	
Involved partners: Chalmers **Authors**: Patrick Moldenhauer, Tobias Mattisson, Peter Hallberg	**Dissemination level:** PU **Nature:** R

Objective

The objective of Work Package 4 is to evaluate the material from Work Packages 1, 2 and 3. The material will be evaluated both with respect to attrition as well as reactivity. This deliverable will report on work performed at Chalmers in T 4.3 with respect to the spray-dried material. The objective is here to confirm the viability and performance of the material selected in WP1 for up-scaling at realistic conditions using a 10 kW CLC unit.

Summary

In Task 1.4 (Deliverable D1.5) a 25 kg batch of spray-dried oxygen carrier material was produced by VITO. The material chosen for the 25 kg batch was based on calcium and manganese doped with titanium and magnesium. The nominal composition is $CaMn_{0.775}Mg_{0.1}Ti_{0.125}O_{3-\delta}$ with a perovskite structure. For Task 4.3, described in this deliverable, the material underwent testing at Chalmers, using a continuous CLC unit designed for 10 kW_{th}. The unit operates at velocities, which are expected in an industrial unit, and thus it is believed that attrition levels could correspond rather well with those in real units. Tests were performed for 193 h hot operation, with 24 h of these with methane. Fuel conversion was monitored for a range of different operational parameters. The loss of fines was monitored, which was the basis of an estimation of the lifetime of the particles of more than 5000 h. The fuel conversion ranged from 50 to 100% and increased with fuel-reactor temperature, specific fuel-reactor bed mass as well as solids circulation. Full conversion of fuel carbon to CO_2 was achieved though at a high specific fuel-reactor bed mass, i.e., approximately 670-1200 kg/MW_{th}.

Contents

1 Introduction

In Work Package 1, a viable oxygen carrier, based on the perovskite calcium manganite and produced with the scale-up ready technology spray-drying is being developed. The oxygen carrier was previously evaluated in the INNOCUOUS project, and has a low attrition rate, and high reactivity towards methane. A large number of these type of materials have been evaluated in this work package using low cost materials and the commercial spray-drying route for production, see Deliverables D1.3 and D1.4. The material selected for scale-up to 25 kg was C28E1S2 with Colormax P of Elkem and Sachtleben TP M211 Hombikat of Sachtleben as sources for manganese and titanium, respectively. The nominal composition was $CaMn_{0.775}Mg_{0.1}Ti_{0.125}O_{3-\delta}$. A batch of 25 kg of material was produced by VITO and dispatched to Chalmers for testing with methane using Chalmers' 10 kW continuous unit. This gas-fired reactor operates using velocities at the nozzles (30-35 m/s) and in the riser (2-3 m/s) that correspond to those expected in a commercial circulating fluidized bed boiler or CFB. The velocities in the cyclone inlet are considerably higher than those in the riser. This means that realistic attrition rates are expected utilizing this reactor unit.

2 Experimental

2.1 Oxygen carrier material

The material examined is based on calcium manganite with a perovskite structure. Small amounts of Mg and Ti were added to this structure to improve fuel conversion, mechanical stability as well as fluidization properties (Mg) [1] and, respectively, inhibit a decomposition of the reactive phases (Ti) [2]. The nominal composition, the source of Mn oxide and Ti oxide as well as calcination time and temperature were selected and optimized in an extensive study [3]. The source of the Mn oxide (Mn_3O_4) was Colormax P of Elkem, which contains about 96 wt% Mn oxide with iron being the main impurity element. As source for the Ti oxide (TiO_2), Sachtleben TP M211 Hombikat of Sachtleben was used, which contains more than 99 wt% of TiO_2 (anatase). The source of Mg was from MgO (Magchem 30, Martin Marietta).

Spherical particles were produced by VITO NV in Mol, Belgium, through spray-drying. The particles were based on the selected C28E1S2-1335, see D1.3. However, in order to achieve sufficient density and strength several batches were produced, with calcination performed at temperatures between 1335°C and 1350°C for 4-16 h. The nominal composition of the material is $CaMn_{0.775}Mg_{0.1}Ti_{0.125}O_{3-\delta}$ and its short denomination is C28E1S2-1335. An XRD analysis was performed at room temperature after the thermal treatment. The crystalline phases identified were mainly $CaMn_{0.9}Ti_{0.1}O_{2.961}$ and a minor amount of MgO. A detailed description of the production of this material can be found in Deliverable D1.5 [4].

Figure 1 and Figure 2 show a light microscope image of the particles and, respectively, a particle size distribution obtained through sieving. Table 1 shows general particle properties.

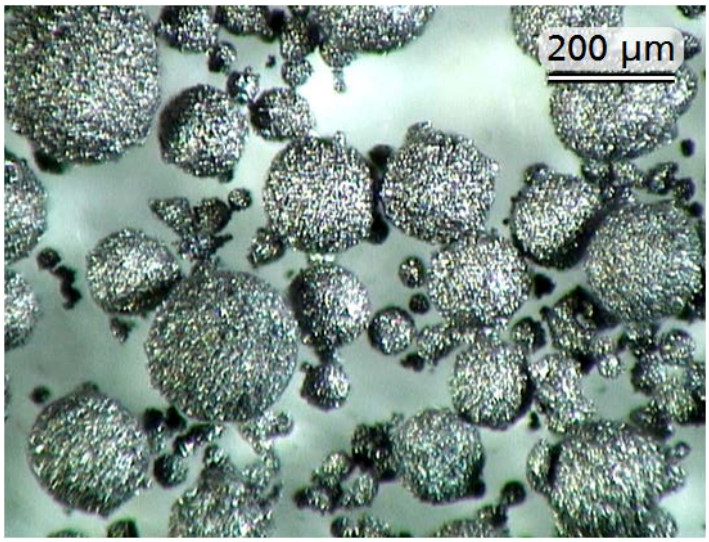

Figure 1: Light microscope image of fresh particles

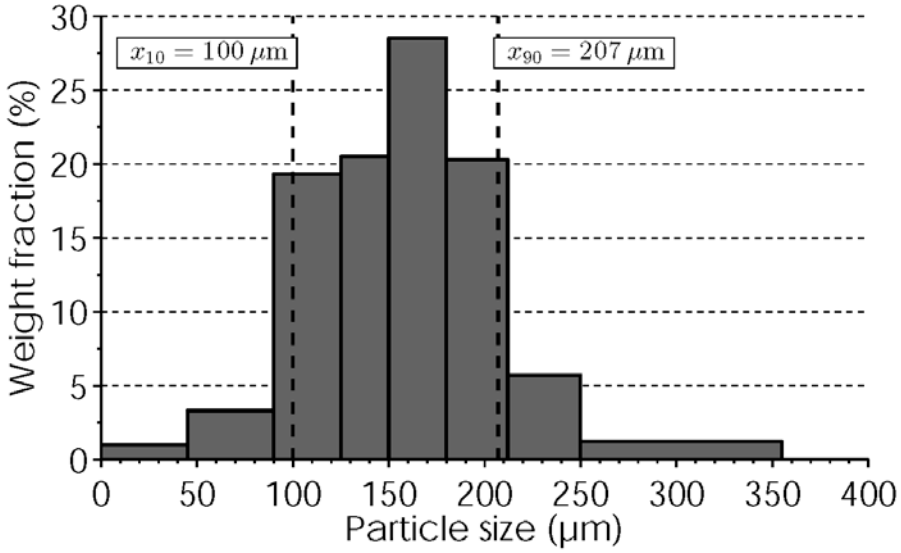

Figure 2: Particle size distribution of fresh particles with distribution points x_{10} and x_{90} visible

Table 1: Properties of fresh oxygen-carrier particles

Parameter	Value	
Bulk density*	1240 kg/m^3	
Harmonic mean size	137 µm†	151 µm‡
Distribution points in particle size distribution§	x_{10} = 100 µm†	x_{10} = 113 µm‡
	x_{90} = 207 µm†	x_{90} = 217 µm‡
Minimum fluidization velocity	1.1 cm/s†	1.3 cm/s‡
Terminal velocity	0.43 m/s†	0.51 m/s‡

* … measured on the basis of standards ISO 3923-1 and ASTM B417

† … based on a particle size distribution obtained through sieving and weighing
‡ … based on a particle size distribution obtained through laser diffraction
§ … 10% of all particles are smaller than x_{10} and 90% of all particles are smaller than x_{90}

2.2 Chemical-looping test unit

The laboratory-scale chemical-looping reactor system reactor system used was constructed in 2002 as part of the GRACE project and has a nominal fuel input of 10 kW_{th}. The first successful demonstration of continuous chemical-looping combustion was performed in this unit. A schematic of the unit is shown in Figure 3.

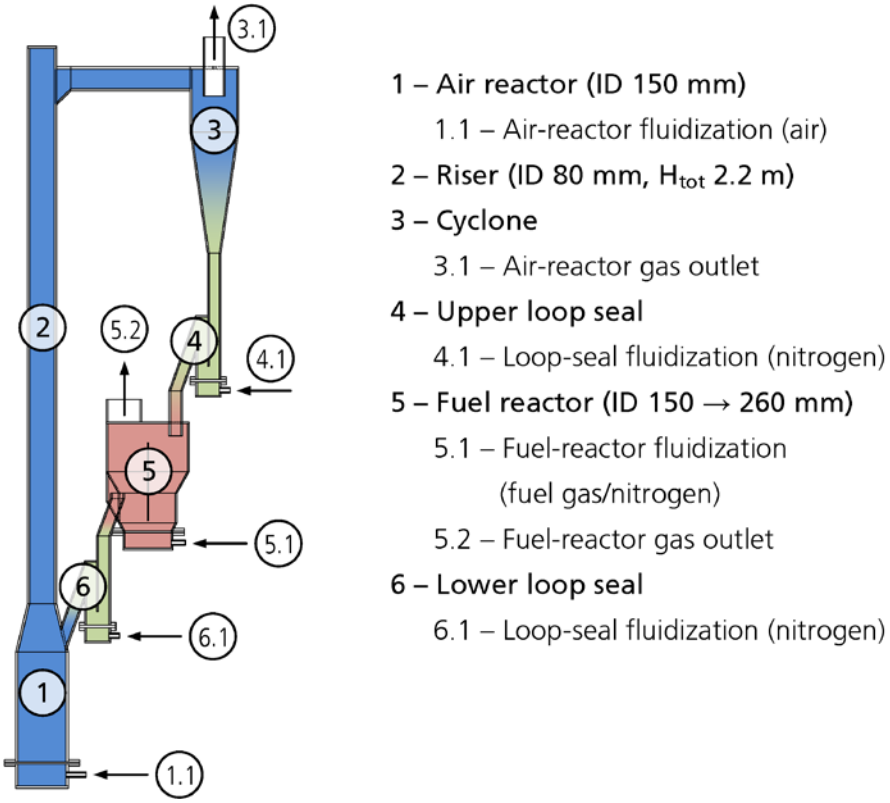

Figure 3: Schematic of the 10 kW chemical-looping combustion reactor

The air reactor (ID 150 mm) tapers down to the riser (ID 80 mm), which drives the global circulation of solids. After the riser, gas and particles are separated in the cyclone. From the cyclone, particles fall down into a loop seal that prevents gas leakage between air reactor and fuel reactor. From the exit of the loop seal, particles flow into the bubbling bed of the fuel reactor. The fuel reactor is equipped with a vertical separation wall to prevent particles from bypassing the bed, see Figure 4. Particles leave the fuel reactor through an overflow exit, which leads the particles, via the second loop seal, back to the air reactor.

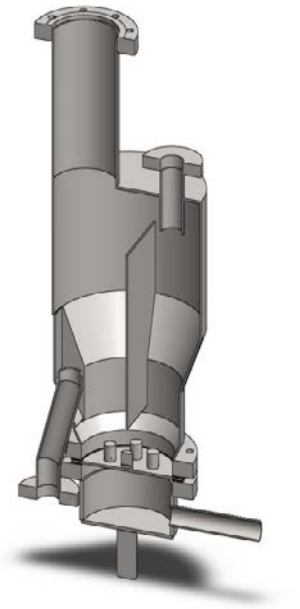

Figure 4: 3D visualization of the fuel reactor with vertical separation wall between particle inlet and outlet.

The flue gases from air reactor and fuel reactor are first passively cooled through finned pipes before sample streams are withdrawn and led to a gas conditioning system. After the gas conditioning system, where the gas is cooled to 4°C and filtered, CO, CO_2, CH_4 and O_2 are measured continuously by infrared and paramagnetic sensors, respectively. Not all particles are removed in the cyclone and, hence, the cyclone off-gas (= the air-reactor flue gas) is led to a bag filter, which captures elutriated particles and fines, before the filtered gas goes to the chimney. The fuel-reactor flue gas passes through a water seal, which has the dual purpose of collecting condensed steam and controlling the pressure in the fuel reactor.

2.3 Experimental parameters

Table 2 shows the main parameters studied in this work. Due to the constant bed height in the fuel reactor, the bed mass here is assumed to be constant. Based on the bed density under minimum fluidization conditions, which is assumed to be 20% lower than the (measured) poured density, and the volume of the fuel reactor below the overflow exit, the bed mass can be estimated. This theoretic bed mass for the particles used here was 2.8 kg, which was also used to calculate the specific fuel-reactor bed mass (fuel-reactor bed mass/fuel input). Pressure measurements in the fuel reactor, however, indicated that the bed mass was as high as 5 kg.

Table 2: Experimental parameters investigated

Parameter	Value
Fuel input (methane)	1.2 – 6.0 kW_{th} (2 – 10 L_n/min)
Fuel-reactor temperature	850 – 980°C
Superficial gas velocity in riser (air)	2.0 – 2.9 m/s (160 – 190 L_n/min)
Solids inventory	≈ 8 – 15 kg
Bed mass in fuel reactor (theoretic)	≈ 2.8 kg
Specific fuel-reactor bed mass*	≈ 470 – 2300 kg/MW_{th}
Total time fluidized under hot conditions (here: > 600°C)	193 h
Total fuel operation time (methane)	24 h

* … Based on theoretic bed mass in fuel reactor, i.e. 2.8 kg, which might be an underestimation.

2.4 Data evaluation

2.4.1 Fuel conversion

The ability of an oxygen carrier to convert fuel to CO_2 is expressed by the CO_2 yield γ_{CO2}, see Equation (1), where $[\,i\,]_{FR}$ are the volume fractions of species *i* measured in the fuel reactor. The calculation is based on a carbon balance over the reactor system.

$$\gamma_{CO2} = \frac{[CO_2]_{FR}}{[CO_2]_{FR} + [CO]_{FR} + [CH_4]_{FR}} \quad (1)$$

The CO_2 yield could of course be dependent upon the degree of oxygen-carrier conversion, which is proportional to the degree of solids recirculation. In this unit the actual circulation cannot be measured directly.

Equation (2) expresses the carbon capture efficiency of the system, i.e., one minus carbon leakage to the air reactor. In Equation (2), $[CO_2]_{AR}$ and $[CO_2]_{atm}$ are the volume fractions of CO_2 measured in the flue gas of the air reactor and, respectively, the atmospheric concentration of CO_2, U_{AR} is the normalized volumetric gas flow in the air reactor and $U_{FR,CH4}$ in is the normalized volumetric flow of methane fed into the fuel reactor.

$$\eta_{CC} = 1 - \frac{([CO_2]_{AR} - [CO_2]_{atm}) \cdot U_{AR}}{U_{FR,CH4\ in}} \quad (2)$$

2.4.2 Oxygen carrier circulation

One way to quantify the circulation of solids in a circulating fluidized bed (CFB) reactor is through the mass flux of solids, G_s, which expresses the circulation as mass flow per area in kg/m^2s. Normally, the cross-sectional area of the riser is used as reference. This allows for comparison of solid circulation of CFB units of different size. It is usually not possible to

measure the mass flux of solids directly, which is why it is calculated based on pressure measurements, which are extrapolated in order to obtain the density at the exit of the riser, ρ_{exit}, see Equation (3) [5].

$$G_{\text{s}} = \rho_{\text{exit}} \cdot (u_0 - u_{\text{t}}) = -\frac{1}{g} \cdot \frac{dp_{\text{exit}}}{dh_{\text{exit}}} \cdot (u_0 - u_{\text{t}}) \quad (3)$$

The following terms are used in Equation (3):

G_{s} (kg/m^{2}s)	mass flux of solids
ρ_{exit} (kg/m^3)	circulating-bed (two-phase) density at the exit of the riser
u_0 (m/s)	superficial gas velocity
u_{t} (m/s)	terminal velocity based on average particle size
g (m/s^2)	gravitational acceleration constant = 9.81 m/s^2
dp_{exit} (Pa)	pressure drop at the exit of the riser
dh_{exit} (m)	height difference of pressure drop dp_{exit}

For practical reasons Equation (3) is simplified and adapted to the 10 kW unit, see equation (4). G_{s}' in Equation (4) is based on a pressure measurement in the middle of the riser. Hence it represents the gross amount of particles, i.e., the sum of particles travelling upwards and downwards, and gives an overestimation of the true mass flux of solids, G_{s}. The estimated mass flux is believed to be proportional to the real mass flux.

$$G_{\text{s}}' = -\frac{1}{g} \cdot \frac{\Delta p}{\Delta h} \cdot (u_0 - u_{\text{t}}) \quad (4)$$

The following terms are used in Equation (4):

G_{s}' (kg/m^{2}s)	estimation of mass flux of solids (gross mass flux of solids)
u_0 (m/s)	superficial gas velocity
u_{t} (m/s)	terminal velocity based on average particle size
g (m/s^2)	gravitational acceleration constant = 9.81 m/s^2
Δp (Pa)	pressure drop in section 2 of the riser (P8-P9)
Δh (m)	height difference of section 2 of the riser = 0.678 m

Equations (5) and (6) show how the superficial gas velocity, u_0, and the terminal velocity, u_{t}, in Equations (3) and (4) are calculated. However, instead of solving Equation (6) directly an approximation is used. For more details see [6].

$$u_0 = \frac{U_{RI}}{A_{RI}} \cdot \frac{T_0 + T_{RI}}{T_0} \quad (5)$$

$$u_t = \left[\frac{4 \cdot d_p \cdot (\rho_s - \rho_g) \cdot g}{3 \cdot \rho_g \cdot C_D}\right]^{0.5} \quad (6)$$

The following terms are used in Equations (5) and (6):

u_0 (m/s)	superficial gas velocity
U_{RI} (m_n^3/s)	normalized volumetric gas flow in the riser
A_{RI} (m^2)	cross-sectional area of the riser
T_0 (K)	reference temperature at normal condition = 273 K
T_{RI} (K)	temperature in riser
u_t (m/s)	terminal velocity based on average particle size
d_p (m)	average particle diameter
ρ_s (kg/m^3)	density of solids
ρ_g (kg/m^3)	density of gas
g (m/s^2)	gravitational acceleration constant = 9.81 m/s^2
C_D (-)	drag coefficient

3 Results and Discussion

3.1 Fuel conversion

Figure 5 shows an overview of the eight experimental days of the test series with the parameters varied and how the performance of the process changed. Complete conversion of methane carbon to CO_2 was achieved on day three at a fuel reactor temperature of 970°C, a circulation index of about 9 kg/m^2s and a fuel input of 4.2 kW_{th}, which corresponds to a specific fuel-reactor bed mass between 670 kg/MW_{th} (based on the theoretic fuel-reactor bed mass) and 1200 kg/MW_{th} (fuel-reactor bed mass based on pressure measurements).

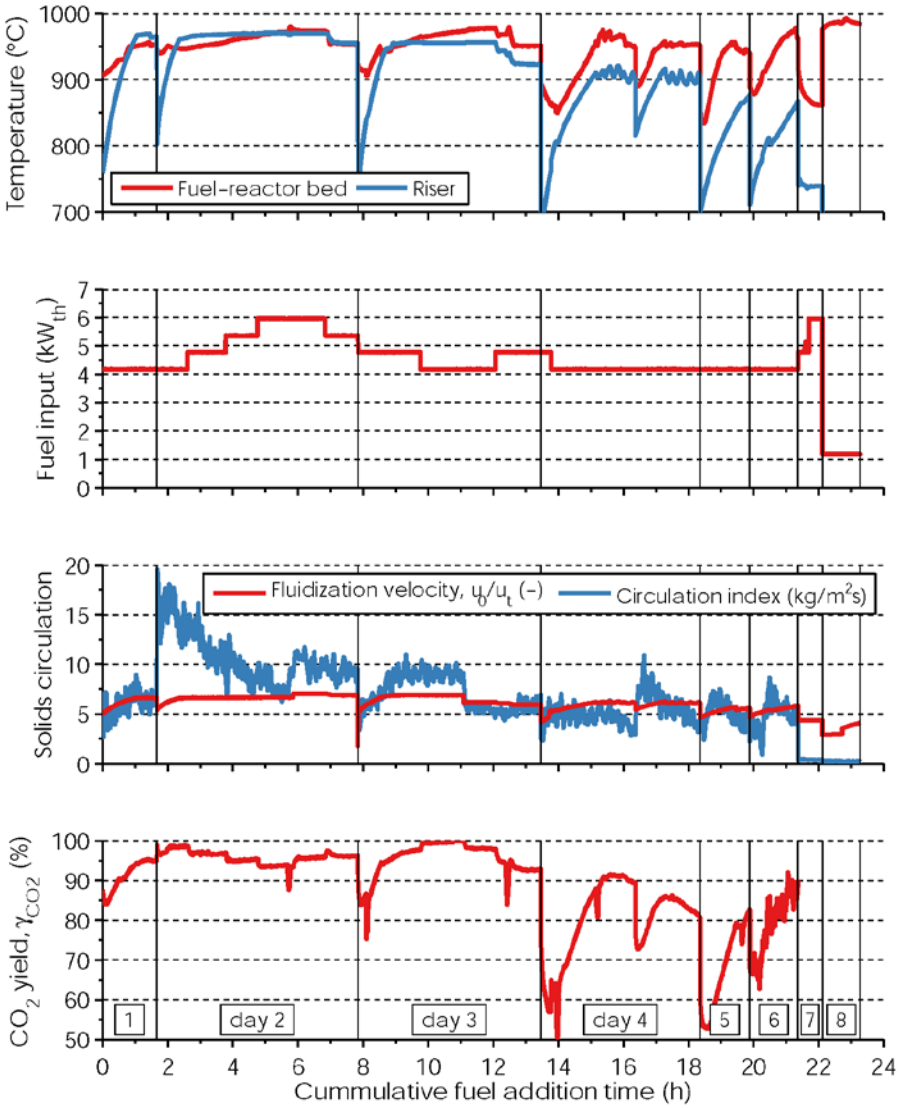

Figure 5: Overview of the parameters varied (temperature, fuel input, solids circulation) and the performance of the process (CO_2 yield, γ_{CO2}). The dimensionless fluidization velocity, u_0/u_t, was calculated with u_t = 0.43 m/s.

Figure 6 shows the CO_2 yield at varied solids circulation at different fuel flows and temperature intervals. The data points form logarithmically-shaped curves and fuel conversion is not much influenced by the solids circulation above a threshold value, i.e., 8-10 kg/m^{2}s, where the gas yield is generally >95%. A slight influence of the fuel input is visible in Figure 6b), where an increase of fuel input causes a decrease in fuel conversion.

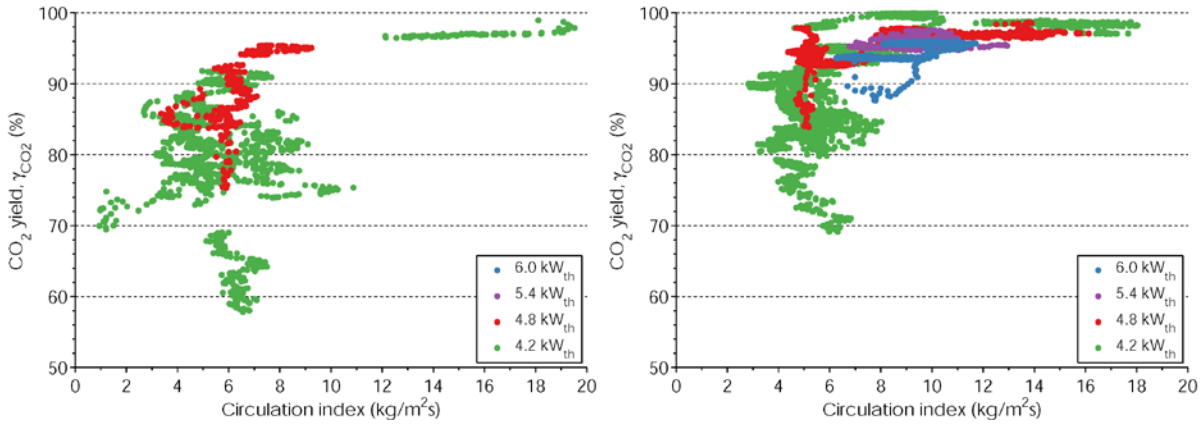

(a) 900-945°C (b) 945-980°C

Figure 6: CO_2 yield at varied solids circulation for different fuel inputs at a fuel-reactor bed temperature of (a) 900-945°C and (b) 945-980°C.

Figure 7 shows the CO_2 yield at varied fuel-reactor bed temperature at different fuel flows and intervals of solids circulation. A clear relation between the temperature and fuel conversion can be seen, which seems to be roughly linear within the interval investigated. Similar to Figure 6b), a slight influence of the fuel input is visible in Figure 7b).

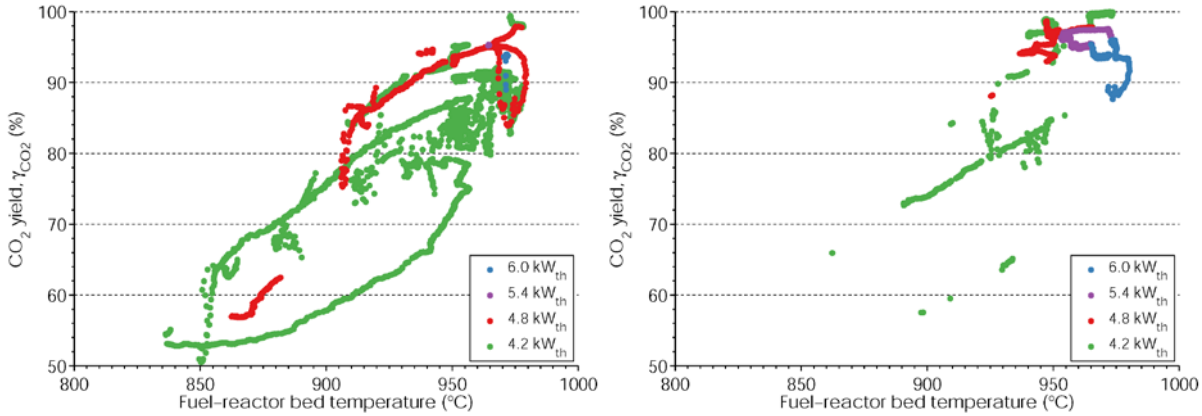

(a) 4-7 kg/m²s (b) 7-18 kg/m²s

Figure 7: CO_2 yield at varied fuel-reactor bed temperature for different fuel inputs at a circulation index of (a) 4-7 kg/m²s and (b) 7-18 kg/m²s.

The concentration of CO_2 in the air reactor was zero throughout the whole test series and, hence, the carbon capture efficiency was 100%. It should be mentioned that the analyzer used to detect CO_2 in the air reactor is not suited for quantifying very small concentrations, i.e., much smaller than 1%.

3.2 Attrition behavior

The off-gas from the cyclone, i.e. stream 3.1 in Figure 3, is cooled and led through a bag filter, where particles and fines larger than 2 µm are captured. Figure 8 shows a quantification of the productions of fines at various points during the experimental campaign. Fines production decreases significantly during the first ten hours of operation. This behavior can be attributed to the production method of the particles, i.e. spray-drying, which is known to produce a varying fraction of hollow particles or donut-shaped particles. These defect particles are prone to breaking during initial operation, which is likely to be the reason for the observed trend.

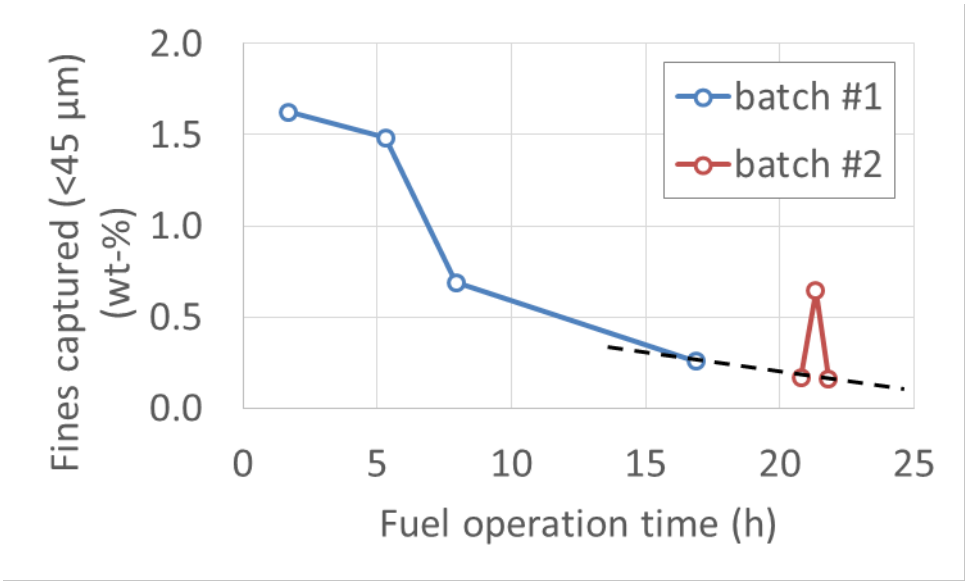

Figure 8: Attrition behavior displayed as percent of fines captured (here: < 45 µm) as a function of fuel operation time

After 20.2 h of fuel operation a fresh batch of particles was used to compensate for material losses (batch #2). At the same time the total inventory was increased from 14 kg to 17 kg. These events are likely to have caused the peak in fine production observed in Figure 8 at around 21 h.

In Figure 8 it is visible that attrition decreases with time even though fine production did not reach a steady state during the course of the experimental campaign. Based on the last points recorded during the experimental a rate of fine production can be assumed, which is visualized as a dashed line in Figure 8. The slope of this line is 0.02 wt-%/h, which corresponds to a lifetime of 5000 h. As fine production most likely would have levelled out if the campaign would have been continued longer, the true lifetime is probably much higher than 5000 h.

The resistance to attrition was quantified with a customized jet-cup attrition rig [7]. The jet-cup attrition rig simulates the grid jets at the bottom of the air reactor/riser as well as the wall friction of the cyclone. Particles in the size range of 125-180 µm were tested with air at ambient conditions. The gas velocity at the inlet nozzle was about 100 m/s. Attrition is

quantified as fines produced in a certain time interval and expressed through the attrition index, A_i, in wt-%/h. The lower the value of the attrition index the higher the resistance towards attrition. Samples of fresh particles and particles captured in the bag filter after 16.9 h were tested in the jet-cup attrition rig. In accordance with the production of fines displayed in Figure 8, the attrition index for fresh particles was higher, i.e. 6.95 wt-%/h, than that for particles after 16.9 h of fuel operation, i.e. 6.00 wt-%/h. However, both values of the attrition index are relatively high for a synthesized material.

3.3 General description of problems during the test series

Initially, the unit was filled with 14 kg of oxygen-carrier material. Pressure measurements indicated that the total inventory diminished steadily, which could be explained only partly by material elutriation, and which was attempted to be resolved by adding more material. The rate of reduction of inventory seems to be lower during the initial days of the experimental campaign than during later ones. After a few experimental days, the unit could not be preheated properly any more, which was attributed to a broken heating cable, which was replaced but failed again. At the end of the experimental campaign, when the insulation was removed and the unit was disassembled, it was discovered that the riser was leaking at several locations. Throughout the campaign, about 30 kg of fresh particles were added to the system (from batch 1 and 2 of C28E1S2-1335 as well as C28 from the INNOCUOUS project), 5 kg were removed in filters and the water seal and about 8 kg were recovered when the unit was disassembled. This means that about 17 kg out of 30 kg left the unit through leaks and likely caused a short-circuit that caused the failure of the heating cables.

Due to the continuously decreasing inventory, the solids circulation could not be kept at a constant level and steady-state operation was achieved only during short periods of time. Even though there was a leakage in the riser, the slight overpressure in the system probably stopped gas from entering the unit. There were no indications that the flue reactor gases were diluted. Even though steady-state operation was not achieved over longer periods of time, the data collected can still be used to assess the fuel conversion properties of the oxygen-carrier material.

Towards the end of the test series, C28 material from the INNOCUOUS project was added to the system in a last attempt to quantify the circulation of solids. At that point it was not clear that there was a leakage of particles. The solids circulation could not be measured successfully and the mixing of the two different materials prohibited that any useful information can be drawn from an analysis of the used material.

4 Conclusions

This deliverable reports on the results of testing a spray-dried calcium manganite-based material that has a perovskite structure. The material was tested at conditions similar to industrial-scale CFB units. Testing at hot conditions (here, more than 600°C) for 193 h, out of which methane was used for 24 h. Complete conversion of fuel was achieved at a fuel reactor temperature of 970°C, a circulation index of about 9 kg/m^{2}s and a fuel input of 4.2 kW_{th}, which corresponds to a specific fuel-reactor bed mass between 670 kg/MW_{th} and 1200 kg/MW_{th}. Based on the data available, the lifetime of the particles is expected to be higher than 5000 h.

References

[1] Hallberg P., Jing D., Rydén M., Mattisson T. and Lyngfelt A. *Chemical looping combustion and chemical looping with oxygen uncoupling experiments in a batch reactor using spray-dried CaMn1- xM xO3-δ (M = Ti, Fe, Mg) particles as oxygen carriers*. Energy and Fuels: 27, pp.1473-1481, 2013.

[2] Leion H., Larring Y., Bakken E., Bredesen R., Mattisson T. and Lyngfelt A. *Use of CaMn0.875Ti0.125O3 as oxygen carrier in chemical-looping with oxygen uncoupling*. Energy and Fuels: 23, pp.5276-5283, 2009.

[3] Jing D., Jacobs M., Hallberg P., Lyngfelt A. and Mattisson T. *Development of $CaMn_{0.775}Mg_{0.1}Ti_{0.125}O_{3-\delta}$ oxygen carriers produced from different Mn and Ti sources*. Materials and Design: 89, pp.527-542, 2016.

[4] Jacobs M., Mattisson T., Lens P., Nicolai S. and Snijkers F. *Deliverable 1.5 - Report on production method and specification of 25 kg batch*. SUCCESS collaborative project, 2016, 8 pages.

[5] Johnsson F., Vrager A. and Leckner B. *Solids flow pattern in the exit region of a CFB-furnace - influence of exit geometry*. in *Fifteenth International Conference on Fluidized Bed Combustion*, Savannah, GA, USA, 1999.

[6] Kunii D. and Levenspiel O. *Fluidization engineering*. 2nd edition 1991, Boston, MA, USA: Butterworth-Heinemann, 491 pages.

[7] Rydén M., Moldenhauer P., Lindqvist S., Mattisson T. and Lyngfelt A. *Measuring attrition resistance of oxygen carrier particles for chemical looping combustion with a customized jet cup*. Powder Technology: 256, pp.75-86, 2014.